DEVELOPMENT OF A PHOTO CATHODE LASER SYSTEM FOR QUASI ELLIPSOIDAL BUNCHES AT PITZ*

M. Krasilnikov#, M. Khojoyan, F. Stephan, DESY Zeuthen, Zeuthen, Germany
A. Andrianov, E. Gacheva, E. Khazanov, S. Mironov,
A. Poteomkin, V. Zelenogorsky, IAP/RAS, Nizhny Novgorod, Russia
E. Syresin, JINR, Dubna, Moscow Region, Russia

Abstract

Cathode laser pulse shaping is one of the key issues for high brightness photo injector optimization. A flat-top temporal profile of the cylindrical pulses reduces significantly the transverse emittance of space charge dominated beams. As a next step towards further improvement in photo injector performance 3D pulse shaping is considered. An ellipsoid with uniform photon density is the goal of studies in the frame of a Joint German-Russian Research Group, including the Institute of Applied Physics (Nizhny Novgorod), Joint Institute of Nuclear Research (Dubna) and the Photo Injector Test facility at DESY, Zeuthen site (PITZ). The major purpose of the project is the development of a laser system capable of producing 3D quasi ellipsoidal bunches and supporting a bunch train structure close to the European XFEL specifications. The laser pulse shaping is realized using the spatial light modulator technique. Laser pulse shape diagnostics based on a cross-correlator is under development as well. Experimental tests of the new laser system with electron beam production are planned at PITZ. First results on the quasi ellipsoidal laser pulse shaping will be reported.

INTRODUCTION

3D shaping of photocathode laser pulses is considered as a next step for further optimization of high brightness photo injectors. Beam dynamics simulations have demonstrated a significant reduction of transverse emittance of electron bunched produced by applying 3D ellipsoidal laser pulses to the rf photo gun [1, 2]. A laser system capable to produce quasi 3D ellipsoidal UV pulses is under development at the Institute of Applied Physics (Nizhny Novgorod, Russia). The Photo Injector Test facility at DESY, Zeuthen site (PITZ) develops high brightness electron sources for modern Free Electron Lasers (FELs) and is intended to be at the site for experimental tests of this system with electron beam production.

The laser system consists of a two-channel fiber laser, a diode pumped Yb:KGW disk amplifier, a 3D pulse shaper and frequency conversion crystals for second and fourth harmonics generation. A scanning cross-correlator system was developed and built to measure spatial and temporal distributions of the laser pulses.

The fiber laser oscillator generates 150 fs pulses at 45 MHz repetition rate. It includes a fiber pulse stretcher, a preamplifier and a system for pulse train (macropulse) formation. A piezoceramic cylinder inside the optical fiber coil of the oscillator is used for precise tuning of the pulse timing to the rf phase of the rf gun. The fiber laser output is splitted into two channels – working and diagnostics. Each channel is supplied with a powerful fiber amplifier. The working channel is used for further amplification, 3D pulse formation and frequency conversion. The diagnostics channel is used to measure the spatial and temporal characteristics of the pulses generated in the working channel. A high speed delay line is implemented in the second channel in order to realize a high precision 3D pulse shape diagnostics. Each channel is supplied with an optical compressor based on a diffraction grating which allows varying the pulse duration within wide range from 200 fs to 100 ps. The compressor of the diagnostic channel is always tuned to the maximum compression down to 200 fs.

The output of the working channel is further amplified by a diode pumped multipass Yb:KGW disc amplifier. 3D shaped pulses are converted into second and fourth harmonics by nonlinear crystals and imaged via the transport beam line onto the photocathode. A splitter before the transport beam line redirects a fraction of the pulse to a cross-correlator.

The paper presents experimental studies performed with different components of the photocathode laser system.

FIBER LASER OSCILLATOR

The fiber laser oscillator has two channels: the channel 1 (CH1) is used for diagnostic of the output laser pulses and channel 2 (CH2) is the working one. Each channel has its own optical compressor with diffraction grating. Linear chirped pulses have ~100 ps duration at the entrance of compressors. The spectra of both channels are centered at 1030 nm and have a width of $\Delta\lambda(FWHM)$=11 nm. A typical spectrum measured at the fiber oscillator output is shown in Fig. 1 (green curve). The optical compressors are based on diffraction gratings with 1200 lines/mm and are capable to compress pulses in each channel down to 200 fs. The maximum average power of the diagnostic and the working channels are P(CH1)=0.912 W and P(CH2)=0.554 W respectively. The pulse train frequency is 1 MHz for each channel and, therefore, the micropulse energies are W(CH1)=0.912 μJ

* The work is funded by the German Federal Ministry of education and Research, project 05K10CHE "Development and experimental test of a laser system for producing quasi 3D ellipsoidal laser pulses".
# mikhail.krasilnikov@desy.de

ISBN 978-3-95450-126-7

and W(CH1)=0.554 μJ. The peak powers of the compressed pulses are 5MW (diagnostic) and 2.5MW (working) [3].

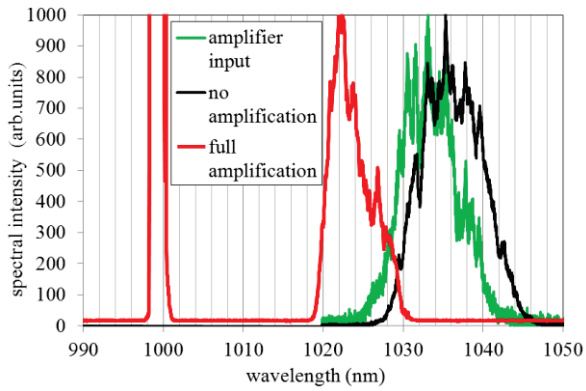

Figure 1: Spectra of the fundamental harmonics: fiber oscillator output (green curve) and measured w/o (black curve) and with full (red curve) amplification.

DIODE PUMPED KGW AMPLIFIER

The pulses from the working channel (CH2) are amplified using a multipass Yb:KGW disk amplifier with a diode pump source LDM 2000-100, which was produced by Laserline GmbH. The concentration of Yb^{3+} in the active elements of the amplifier is ~3%. The crystal is cut as a rectangular, L_x- length is 7 mm, L_y-width is 7 mm and L_z–thickness is 3 mm. The axis orientation is $N_m||L_x$, $N_p||L_y$ and $N_g||L_z$ correspondingly. The entrance surface is coated for high transmission of the pump (935 nm) and signal (1030 nm) optical pulses, the back side of the crystal is coated for high reflection at these wavelengths.

Two laser heads are installed in the Yb:KGW amplifier which allows 5 V- and 4 V- passes in the first and the second active element. The setup of laser heads implies imaging of the first active element onto the surface of the second one.

A transverse distribution of the diode pump power is shown in Fig. 2. The distribution is rather symmetrical and is well matched in size to the amplified pulse from the working channel. The diode pump pulse has a flattop shape with 2.5 ms FWHM and 0.3 ms rise and fall time.

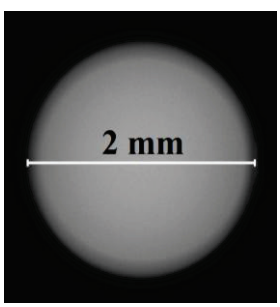

Figure 2: Transverse distribution of the diode pump power.

The internal absorption of the pump radiation inside the active element plays a significant role in the amplification process. The absorption of a single V-pass has been measured. The polarization of the pumping pulse was chosen parallel to *m* and *p* axis. The wavelength of the pump radiation was varied by means of cooling water of the diode pump. It has been found that the absorption shows some increase for both polarizations with a temperature increase.

The absorption coefficient of the pump radiation at 30˚C with E||m polarization is almost 90% whereas for the E||p polarization it is ~27%. These measurements are in a good agreement with earlier published reference data.

The laser oscillator center wavelength of 1045 nm is offset by +5+7 nm from the KGW bandwidth (λ=1028-1030 nm). The amplification shifts the center wavelength towards the maximum of the amplification. That is why the fiber laser oscillator was replaced with another oscillator with center wavelength at 1032 nm. Due to the nonhomogeneous amplification spectrum the center wavelength is shifted to 1035 nm. However, in the case of strong amplification the crystal absorption spectrum is being strongly modified and the center line is strongly shifted to 1022 nm (Fig. 1).

The amplification on the KGW crystal is characterized by a strong enhancement of the spontaneous luminescence. The maximum intensity of the amplified spontaneous radiation (ASR) was observed around λ=1000 nm. A strong enhancement of the ASR is shown in Fig. 1 (red curve). The ASR impact onto the time resolved measurements was detected as an increased background of the macropulse (Fig. 3). A photodiode with slow time response was used to measure these time dependencies. This explains the strong distortion of the macropulse edges.

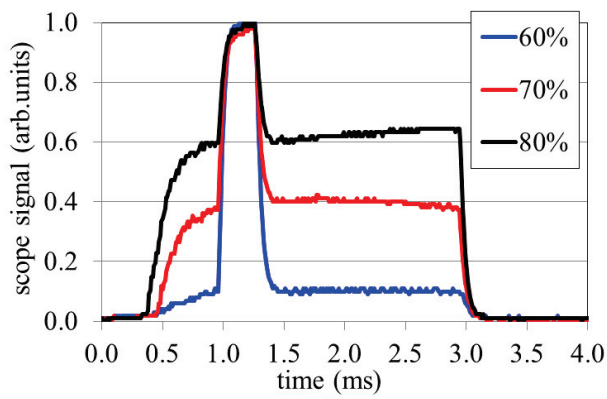

Figure 3: Scope signal of the KGW amplifier output. The main signal (1.0 – 1.3 ms) is strongly polluted with ASR background. Values of the legend correspond to the amplifier power level (2000 W was measured at 100%).

As it can be seen from Fig. 3 the ASR energy is significantly higher than the pump energy already at 80% of the full pump power (~1600 W). The amplified signal was not observable at 100% pump power level (~2000 W). In order to reduce this unwanted effect a

ISBN 978-3-95450-126-7

spatial filter was applied to narrow the radiation spectrum. An opaque mask with 8 holes was installed in the focal plane of the amplifier telescope. Modeling of the amplifier with such a mask yielded the minimum size of the mask holes of 4.5 mm. This implies a reduction of the acceptance angle by a factor of 13 and the ASR power is reduced by a factor of ~170, but the distortion of the transverse distribution is still acceptable. Nevertheless, this will still not be sufficient for the 100% pump power level. Further reduction of the hole size (<4.5 mm) will allow amplification almost without ASR production, but as a drawback the filtering of the high frequency spatial harmonics will result in a less sharp border of the 3D ellipsoidal pulse. Beam dynamics simulations to study the influence of the cathode laser border sharpness onto the electron bunch emittance have been performed [2].

Experimental studies yielded 15-20% ASR level w.r.t. to the main macropulse energy obtained for 3 mm holes. In this case all high frequency components were cut (Fig. 4a, b). However such reduction of the acceptance angle allowed the full amplification (after a double-pass) resulting in a micropulse energy of 120 μJ (Fig. 5). It should be noticed that this pulse energy level was measured without pulse shaping, which in turn will lead to additional losses.

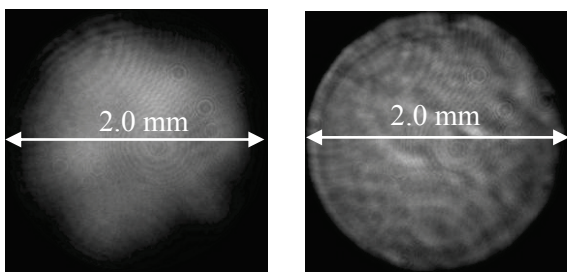

Figure 4: Transverse distribution of the KGW diode pump power: without spatial filter (left) and using a mask with 3 mm holes (right).

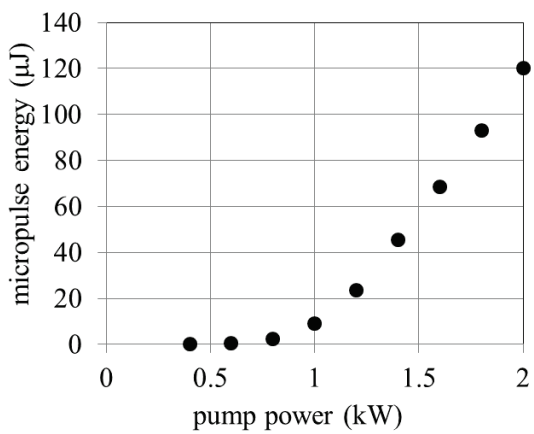

Figure 5: Dependence of micropulse energy after the amplification on the pump intensity.

As another option a selective frequency filter transparent for λ=1022 nm and cutting ASR signal (λ=1000 nm) is under consideration as well.

The output signal from the Yb:KGW amplifier is imaged by means of Kepler telescope lenses onto the frequency conversion LBO crystal. The experimental optimization of the second harmonic frequency generation resulted in a ~20% efficiency for a 7 mm thick LBO crystal and 20 ps (FWHM) laser pulses with 24 μJ (fundamental wavelength). No saturation was observed for the second harmonic generation. Further intensity increase and usage of a chirped prism for the fundamental harmonic allowed achieving a ~70% conversion efficiency.

3D PULSE SHAPING

In order to produce quasi ellipsoidal laser pulse a 3D pulse shaper was developed and tested. Its principle is shown in Fig. 6. Currently an experimental setup uses 100% reflective mirrors instead of Spatial Light Modulators (SLMs). This simplification is not essential in terms of linear losses, high frequency harmonics transmission and astigmatism, but it allows to avoid the instability of the SLM reflectivity (described below).

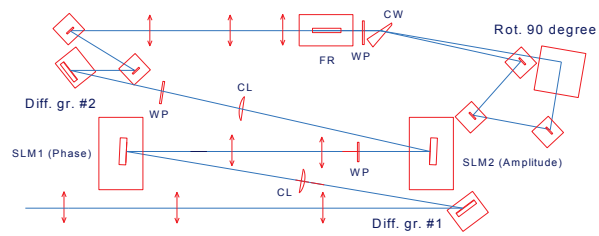

Figure 6: Setup of the 3D pulse shaper: Diff. gr. – diffraction gratings, SLM – spatial light modulator, WP – half-wave plates, CL – cylindrical lens, FR – Faraday rotator, CW – calcite wedge, Rot. 90 degree – rotator of the laser beam by 90 degree.

The pulse shaper is based on a zero dispersion optical compressor. It consists of two diffraction gratings, two single Kepler telescopes with cylindrical and spherical lenses and two liquid crystal based SLMs. The modulators are located at the focal plane of the telescope made of cylindrical lenses which images one diffraction grating onto the other in the meridian plane (plane of the sketch in Fig. 6). There is no such imaging in the sagittal plane which implies corresponding diffraction. However, these effects are not substantial for laser beams of 8 mm diameter focused by a cylindrical lens with a 405 mm focus. Telescope with spherical lenses images one SLM onto the other. The first SLM manipulates the phase of the laser pulse. A half-wave plate is installed before the second SLM. This introduces a 45 degree rotation of the laser pulse polarization and therefore the second SLM becomes an amplitude manipulator.

ISBN 978-3-95450-126-7

The laser pulse is passing through the pulse shaper twice (Fig. 6). The first pass forms the laser profile in the meridian plane and time, the second pass after a 90 degree rotation is responsible for the pulse shaper formation in the sagittal plane and time. In order to study pure impact of the optical system onto the transverse distribution of the laser pulse, the SLMs were replaced by mirrors. These tests did not reveal any significant distortions in the transverse laser spot. A transverse distribution of the laser pulse after double pass through the pulse shaper is shown in Fig. 7.

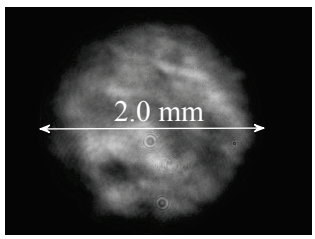

Figure 7: Transverse distribution of the shaped laser pulse.

A single pass through the pulse shaper has a linear transmission of ~30%. The losses are partially compensated by return pass through the Yb:KGW amplifier. However the maximum attainable energy of a micropulse is ~31 μJ which is factor ~4 lower than without pulse shaper.

The HES 6010 NIR SLM produced by Holoeye Photonics AG (Germany) is used for the pulse shaper tests. According to the technical certificate its reflection must not go below 60%. The measurements gave a value of 72% for horizontal polarization, required for the realized diffraction grating. But this value is a result of a rather long term averaging. At the ms time scale (Fig. 8) the signal after the SLM acquires a strong noise [4]. The noise amplitude depends on the voltage applied to the SLM (Fig. 9). This unexpected SLM property complicates the pulse shaping significantly. One of the possible solutions of the problem is the implementation of cooling of the SLM screens with a Peltier cooler. This approach resulted in some reduction of the SLM noise level by a factor of 2 in amplitude. An additional complicated cooling setup yielded noise reduction by a factor of 4, but efficient cooling requires rather complicated construction efforts, and it was not possible to keep this sophisticated setup working for more than a few minutes. After a short time the SLM surface became covered with frost and lost its optical properties. In-vacuum SLM housing can probably improve the cooling but it requires significant design and construction efforts.

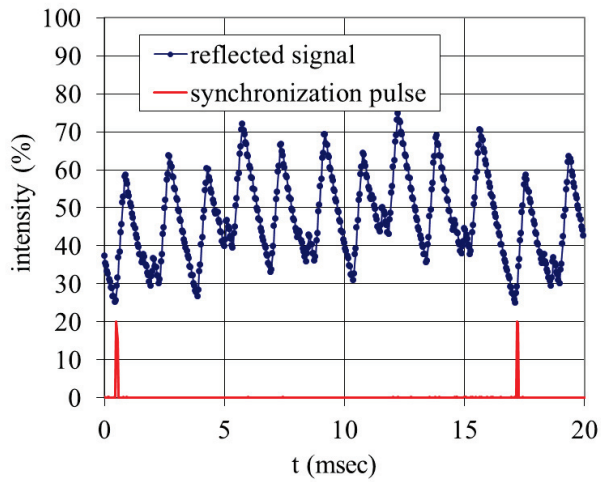

Figure 8: Time evolution of the SLM reflectivity. Synchronization pulses from the SLM are shown on the top of the horizontal axis.

As a solution of the modulator phase noise problem a SLM with a thicker liquid crystal matrix was suggested by the SLM producer (Holoeye Photonics AG). Corresponding tests were performed, but only a factor of 2 in the noise reduction was obtained (solid curve in Fig. 9), which is still far from the wanted phase stability level.

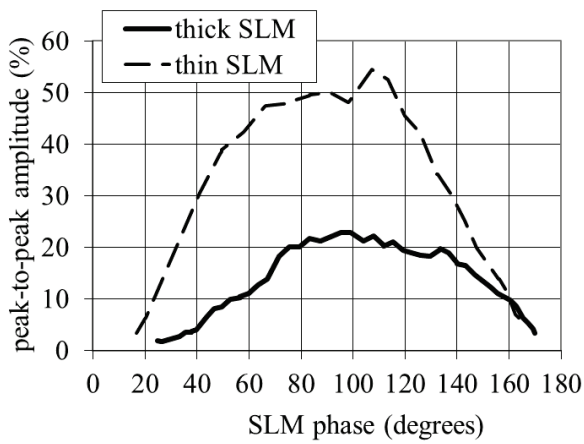

Figure 9: Peak-to-peak noise amplitude of the signal reflected from the SLM as a function of the modulator phase (SLM voltage). Dashed line corresponds to measurements with a thin SLM matrix, the solid cure was obtained using a thick matrix.

Another approach to reduce the observed SLM phase noise can be based on precise synchronization of the input laser signal to the phase of the SLM (Fig. 8). This method cannot be integrated in the photo injector timing system, but it makes possible to perform experimental studies on the working point of the 3D pulse shaper.

SCANNING CROSS-CORRELATOR

In order to implement precise measurements of the temporal structure of 3D ellipsoidal laser pulses a

ISBN 978-3-95450-126-7

scanning cross-correlator (SCC) was developed. Short pulses from the diagnostic channel (CH1) of the fiber laser oscillator are involved in the SCC. The length of these pulses corresponds to the Fourier limit.

A BBO crystal with 1 mm thickness is used for the nonlinear second harmonic generation from the non-collinear pulses overlap using varying time delays [5]. A cross-correlation function obtained as a dependence of the second harmonics energy on the delay time assuming small conversion efficiency (0.1% in the experiment) contains the information about the time structure of a pulse in the working channel (CH2). A 3D modeling of the SCC yielded a tolerance on the angle misalignment of 2.5 mrad.

Fig. 10 illustrates the working principles of the scanning cross-correlator. The major challenge for the SCC development was a high scanning speed determined by the macropusle duration (T=300 μs). A working laser pulse with t_m duration has to be scanned by a short diagnostic pulse of t_d length during the macropulse. Including margins to the working pulse duration implied a measurement window $t_w > t_m$ (Fig. 10) within which the scanning has to be performed.

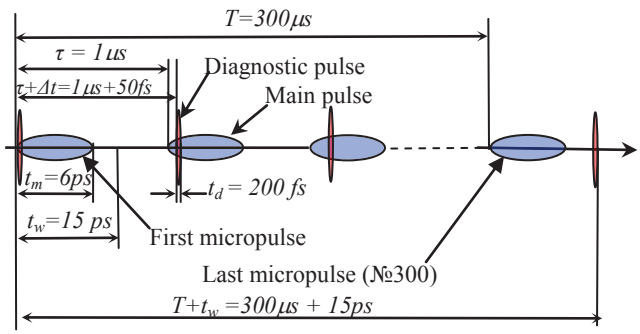

Figure 10: Time scheme of the scanning cross-correleator for 3D pulse diagnostics.

The minimum time resolution of the SCC is determined by the number of pulses in a macropulse N=300. A time step of the scanning procedure is $\Delta t = t_w / N$ =50 fs. This is an estimation of the lower limit of the time resolution under assumption of an infinitely short diagnostic pulse.

The delay of the working pulse w.r.t. the measured pulse has to be t_w within the macropulse duration T. Therefore the speed of its delay in space has to be $V = ct_w / T = 1500$ cm/s, where c is a speed of light. Moreover this speed should not vary during scanning time t_w.

In reality the time resolution is stronger impacted by the finite length of the diagnostic pulse which is close to the Fourier limit and is ~200 fs. Thus, the time resolution is about factor 4 worse than Δt =50 fs. But the scanning speed still has to be as high as 1500 cm/s.

The delay line of the developed SCC is based on a single mode polarization-maintaining (PM) optical fiber of 80 m length wound on a thin piezoceramic cylinder [6]. Applying a sawtooth voltage (0-400 V) to the cylinder leads to a fiber length variation. This allows scanning of the working pulse within 300 μs at a constant speed of 1500 cm/s. Tests of the developed SCC were performed for a speed range from 4 cm/s to 1600 cm/s. The calibration was realized using an external micrometer air delay line.

The linearity of the scanning speed within the scanning window is a key characteristic of the cross-correlator. Despite rather smooth variation of the drive voltage applied to the piezoceramic cylinder, it spectrum width is wide enough to excite mechanical resonances within the system resulting in fluctuations of the scanning speed. These fluctuations were measured using the external air delay line. Fig. 11 shows the time dependence of the scanning speed measured at the maximum speed of the drive voltage variation (400 V/ms). The scanning speed variation is $\Delta V / V = \pm 8\%$ for a 52 ps scanning window, $\Delta V / V = \pm 1.5\%$ - for 30 ps and $\Delta V / V = \pm 0.5\%$ - for 15 ps.

The maximum achieved scanning speed of 1600 cm/s allows performing measurements within a 16 ps window using 300 μs macropulse. Assuming 200 fs duration of a diagnostic pulse yields 50 time samples for the measurement within this window.

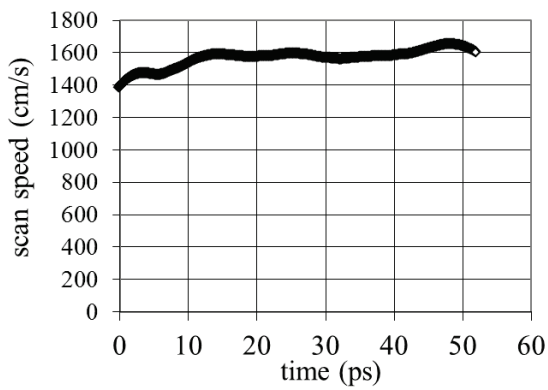

Figure 11: Time dependence of the scanning speed measured at the maximum speed of the drive voltage variation (from 0 to 400 V in 1 ms).

FIRST MEASUREMENTS

A simplified 3D pulse shaper setup for quasi ellipsoidal pulse generation was tested using the scanning cross-correlator. Linear chirped laser pulses with a 40 ps length and 11 nm bandwidth were used for preliminary experiments. The amplitude mask only was applied to form the pulse shape. The measured profile of the fundamental harmonic pulse is shown in Fig. 12. The possibility to utilize a pulse train with 1 MHz pulse repetition frequency and 300 μs macropulse length to characterize picosecond pulses was successfully demonstrated. A time resolution of ~200 fs was achieved for the measurement window of 50 ps. The principle ability to generate quasi ellipsoidal laser pulses was demonstrated.

ISBN 978-3-95450-126-7

The developed scanning cross-correlator has to be combined with a fast camera (~30000 frames/s). This should enable not only temporal profile measurements but also full 3D pulse shape characterization.

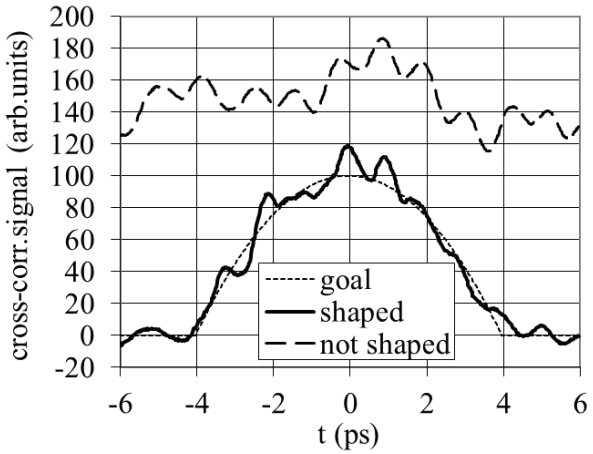

Figure 12: Profiles of the measured cross-correlator function: upper dashed line – no pulse shaper applied, solid line corresponds to the amplitude mask applied to form the quasi ellipsoidal pulse and additionally a theoretical profile of the ellipsoidal pulse (dotted curve).

SUMMARY

Quasi ellipsoidal cathode laser pulses are considered as a tool for further optimization of high brightness electron sources required for modern FELs. A laser system capable of 3D pulse shaping is currently under development at IAP (Nizhny Novgorod, Russia) and planned to be tested with electron beam production at PITZ (DESY, Zeuthen site).

Major design specifications of the laser system are achieved. The fiber laser oscillator works at a center wavelength of 1030 nm and generates pulse trains with up to 300 μs length at 1 MHz pulse frequency and up to 10 Hz repetition rate. The micropulse duration is variable within a range from 0.2 ps to 100 ps, the pulse energy is up to 0.55 μJ. A multipass Yb:KGW disk amplifier with a diode pump is capable to increase the micropulse energy up to 120 μJ. The demonstrated efficiency of the second harmonic generation is ~20%, it is planned to increase it up to 70% by intensity tuning and usage of a prism for angular chirp. This should also allow a high efficiency of the fourth harmonic generation.

A scanning cross-correlator was developed and tested. The scanning speed of 1600 cm/s allows performing detailed measurements of the temporal and spatial characteristics of ellipsoidal laser pulses with a time resolution better than 300 fs within the time window of up to 50 ps.

First tests of the 3D pulse shaper and the scanning cross-correlator demonstrated generation of quasi ellipsoidal laser pulses of the fundamental harmonic.

A production of quasi ellipsoidal UV laser pulses with micropulse energy >10 μJ and 7 ps rms pulse duration is considered as a next step in the ongoing development.

ACKNOWLEDGMENT

The work supported by the German Federal Ministry of education and Research, project 05K10CHE “Development and experimental test of a laser system for producing quasi 3D ellipsoidal laser pulses” and RFBR grant 13-02-91323. The authors thank M. Groß for reading the paper and giving valuable feedback.

REFERENCES

[1] M. Krasilnikov et al., “PITZ Experience on the Experimental Optimization of the RF Photo Injector for the European XFEL”, TUOAN004, FEL2013.

[2] M. Khojoyan et al., “Beam Dynamics Optimization for the High Brightness PITZ Photo Injector Using 3D Ellipsoidal Cathode Laser Pulses," TUPS036, FEL2013.

[3] E. A. Khazanov et al., "Cross-Correlator for the Diagnostics of 3D Ellipsoidal Shaped UV Laser Pulses for XFEL Ultra Low-Emittance Photoinjector," in CLEO: 2013, OSA Technical Digest (online) (Optical Society of America, 2013), paper JTh2A.27.

[4] A. Farre et al., “Positional stability of holographic optical traps," Optics Express, Vol. 19, Issue 22, pp. 21370-21384 (2011).

[5] V. Zelenogorsky et al., “Scanning cross-correlator to monitor 3D ellipsoidal laser pulses," Quantum Electronics, 2013 (in Russian), to be published.

[6] Gelikonov V.M et al., Instruments and Experimental Techniques, **53**(3), 443-446 (2010).

ISBN 978-3-95450-126-7